Hittite Journal of Science and Engineering, 2019, 6 (2) 99-107
ISSN NUMBER: 2148-4171
DOI: 10.17350/HJSE19030000134

Methodology on Co-Registration of Mri and Optoelectronic Motion Capture Marker Sets: In-Vivo Wrist Case Study

Senay Mihcin
Katip Çelebi University, Biomedical Engineering, İzmir/Turkey

ABSTRACT

Skin-surface mounted markers provide incomplete spatial information of the underlying-bone. A new methodology is developed combining optoelectronic motion capture (MOCAP) and imaging modalities to co-register the positions of underlying-bone and external markers. Skin surface-mounted markers, utilized in MR imaging, were coated with reflective material to collect spatial data in passive infra-red optoelectronic MOCAP system. Two-link jig mechanisms were designed to mount-on marker sets; these were rotated in increments through 180° of angular rotation at pre-determined angles. The rotations were recorded within the MOCAP system and 3T MRI scanner under a 3D STIR (short tau-inversion recovery) sequence. A 3D in-silico model was built for the co-registration of marker centroids' on a 1 to 1 scale. Differences were calculated from the co-registered data obtained from these two systems using the same set of markers. Root mean square error (RMSE) and angular rotation was less than 1.5 mm in translation and 1° respectively in-vitro. Concordance Correlation Coefficients (CCC) was calculated as (0.9788 to 1). Mean-Difference plots showed good agreement. Next, adduction/abduction movements of the natural wrist joint were investigated in six healthy subjects. MOCAP data was collected for three sets of motions, and MRI scans were repeated twice to derive within-subject repeatability data. Within-subject, the maximum RMSE for wrist angular rotations was 1.28° and 1.30° respectively in vivo. Pearson correlation coefficient was calculated for adduction and abduction as 0.70 and 0.71 respectively. Paired Student-t test identified systematic differences. The used methodology established the way to analyze the relationship between the bone and external markers.

Article History:
Received: 2018/07/15
Accepted: 2019/02/04
Online: 2019/06/30

***Correspondence to**: Senay Mihcin, Katip Çelebi University, Biomedical Engineering, İzmir, TURKEY*
E-Mail: senaymihcin@ikc.edu.tr
Phone: 0232 329 37 61

Keywords:
Joint angle; Optoelectronic motion capture systems; Cross sectional imaging modalities; Image registration; Wrist kinematics.

INTRODUCTION

The measurement of human kinematics is underpinned by the need to isolate and model the movement of bony segments [1]. Advances in the study of human kinematics are challenged however by the difficulty of measuring skeletal movement using surface mounted markers [2]. One of the major confounders in this field is soft tissue movement artefact (STA), caused by differential movement of the skin-mounted markers relative to the underlying bones [3]. Although alternative techniques exist that incorporate direct modelling of the internal structures, such as stereo radiography and single plane fluoroscopy, as well as measurements derived from bone pins or external fixation devices [4,5,6,7], these methods are either invasive or expose the subject to ionizing radiation. Mundermann et al [8] suggested markerless motion capture for lower limbs. Although this would represent a non-invasive and non-constraining method, it also requires drawing of inference for internal structures from surface measurements. Also for very complicated joints such as the spine, the accuracy and relevance remains uncertain and the technique is not at the stage of application for clinical purposes.

For some anatomical regions such as the talus in the hind foot and the spine, the anatomy is either not accessible from the surface or is functionally too complex to relate surface mounted marker outputs to the underlying bony segments reliably. In this study, I explored the feasibility of a combined approach in which the coordinates of reflective coated, surface-mounted-MRI-marker set can be mapped explicitly onto the underl-

ying anatomy using internal imaging, as a first step towards clinical applications for subject specific implant modelling. Andriacchi et al. [9], described briefly a similar methodology for understanding knee kinematics, but the work was aimed at generating animations and no substantive quantitative results were reported. A recent report by Andersen et al [10] investigated the accuracy of a linear STA model in human movement analysis by simultaneously recording bone-mounted pin and skin marker data for the thigh and shank using bi-planar radiographs for walking, cutting and hopping. However, without use of the cortical bone pins, the problem of STA still remains challenging and our study aimed to identify whether a non-invasive solution might be achievable.

The specific aims of the current study were i) to establish a methodology for the proof of concept and to quantify the error associated with the co-registration of the two data sets; as surface marker data in (MOCAP) and surface marker data in (MRI) in vitro model and ii) once proof of concept was established, to determine the error associated with the technique in the natural wrist joint, for co-registration of the surface markers (MOCAP) and (MRI) universes and for the relationship of the surface markers to the underlying segmented bone data (MRI).

MATERIAL AND METHODS

In-Vitro Phase

Twelve surface markers were attached to a purpose built jig mechanism consisting of two links and a revolute joint which was constructed from polyethylene and fixed to a base produced from a polyamide (nylon) composite material (DuraForm, 3D Systems) (Fig. 1). The base of the jig was manufactured using a Vanguard Selective Laser Sintering Rapid Prototyping machine (Sinterstation HIQ Series, 3D Systems, Valencia, CA) and contained a grid of internal calibration channels with a diameter of 6.4 mm filled with saline water for warping investigation of MRI images. The hinge mechanism of the two links was designed to represent a highly constrained planar movement, as a simplified representation of radial-ulnar deviation of wrist joint.

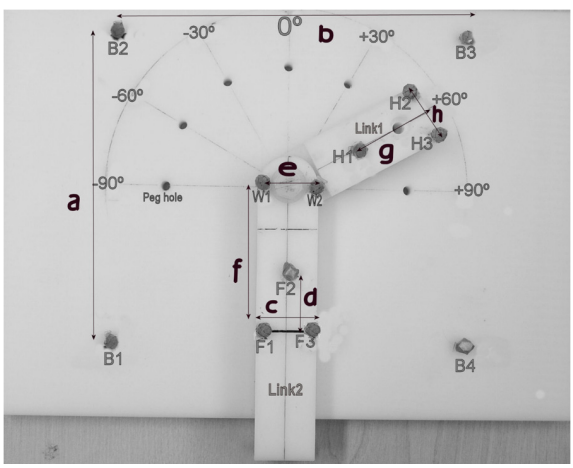

Figure 1. Two-link mechanism with a grid surface base filled with saline water with 6.4 mm diameter holes securely fitted at the ends and at the angle of +60° degrees for Link1
Dimensions of the field of view for MRI

a=160 mm	c=30mm	e=30mm	g=30mm
b=160mm	d=30mm	f=80mm	h=30mm

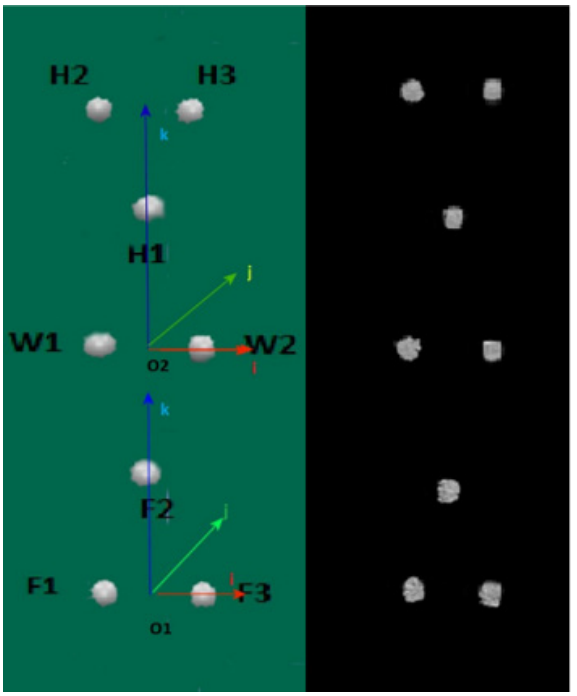

Figure 2. Markers in a) the motion capture system (MOCAP) showing the reference frames on two segments and in b) the MRI system, with Link 1 aligned at 0°in both cases.

The twelve 6mm PinPoint® markers (Beekley Corp., CT, USA) were attached to the jig in the configuration illustrated in Fig. 1. The markers consisted of spherical balls, filled with a proprietary fluid (Radiance ®) which generates high signal on MRI. Prior to use, markers were also coated with retro-reflective material to enable their use with the passive infra-red reflective marker motion capture system. The markers were positioned as follows: four markers (B1, B2, B3, B4) were placed to serve as a local coordinate system for the base, three tracking markers were placed on each of the fixed (F1, F2, F3) and rotating links (H1, H2, H3) and two calibration markers (W1, W2) were placed at each side of the revolute joint representing the wrist (Fig. 2 a and b).

Experimental Protocol in Vitro

Link1 on the jig mechanism (Fig. 1) was adjusted to rotate around the revolute joint through 180° in seven increments, with a peg-and-hole arrangement precision mac-

hined into the jig at 30° intervals to ensure consistency of positioning. Marker data for each position was captured using both a 3D passive marker motion analysis system (Vicon MX, Oxford Metrics, UK) and an MRI scanner (Siemens Magnetom 3 Tesla MRI using 3D voluming), as detailed below.

The MOCAP system used in this study was a part of GAIT laboratory for clinical studies in a hospital which consisted of eight passive-marker cameras (Vicon MX with T40 cameras, Oxford Metrics, UK) capturing at 150 Hz and 2 Mega-pixel resolution. The system is installed for regular patient examination. It is installed and according to the quality management regulations of the hospital. The cameras have 6.5-15.5 mm Varifocal lenses. Technical error for the cameras within a working volume of 10 x 11 x 2.5 m was calculated as less than 0.2 mm for this experimental set-up. The motion analysis data were acquired using Vicon Nexus 13.1 and transferred to Visual3D software (C Motion, Germantown, MD) for initial post processing.

The jig was then transferred to the MRI suite where imaging was performed using a 3T Siemens Magnetom Verio scanner with a 32 channel body coil. The images were acquired using a 3D SPACE sequence (TR=540ms, TE=108ms, 0.85mm isotropic resolution). The grid surface of the test rig was initially assessed for residual warping after a proprietary distortion correction algorithm, built into the scanner's standard software, had been applied. The standard deviation of the measured dimensions from the known dimensions was calculated as 1.01 mm in the X direction and 1.07 mm in the Y direction over the whole field of view (160 mm by 60 mm) after application of the distortion correction algorithm. This algorithms was applied to all subsequent image datasets. The fixed link (Link2) was aligned with the long axis of the MRI coil co-centrically. As with the motion analysis data capture, Link1 was sequentially rotated in constrained 30° increments through the 180° range of motion and the jig was imaged at each increment.

In-Vivo Phase

Participants

The right wrists of six healthy subjects (3male and 3 female, average age of 34 in the range of 31- 45) were investigated in this study. The subjects had no history of wrist injury. Ethical committee permission was obtained from university's ethics committee, and written consent was obtained from all participants prior to their involvement in the study.

Experimental Protocol in Vivo

A revised experimental jig was designed so that the subjects could place their forearms in three constrained positions representing adducted, neutral and abducted positions of the wrist (Fig. 3a). This jig consisted of a resting surface with a peg and a hole mechanism to place the hand in the pre-determined positions. At the wrist and along the forearm, supporting pegs and Velcro bands secured the forearms of the participants for stability.

Optoelectronic motion data was initially gathered from the participants at the gait lab (Fig. 3b) with the markers placed on wrist in the same configuration using the Vicon system as defined previously for the in-vitro phase. Static and dynamic coordinates of the markers derived from the

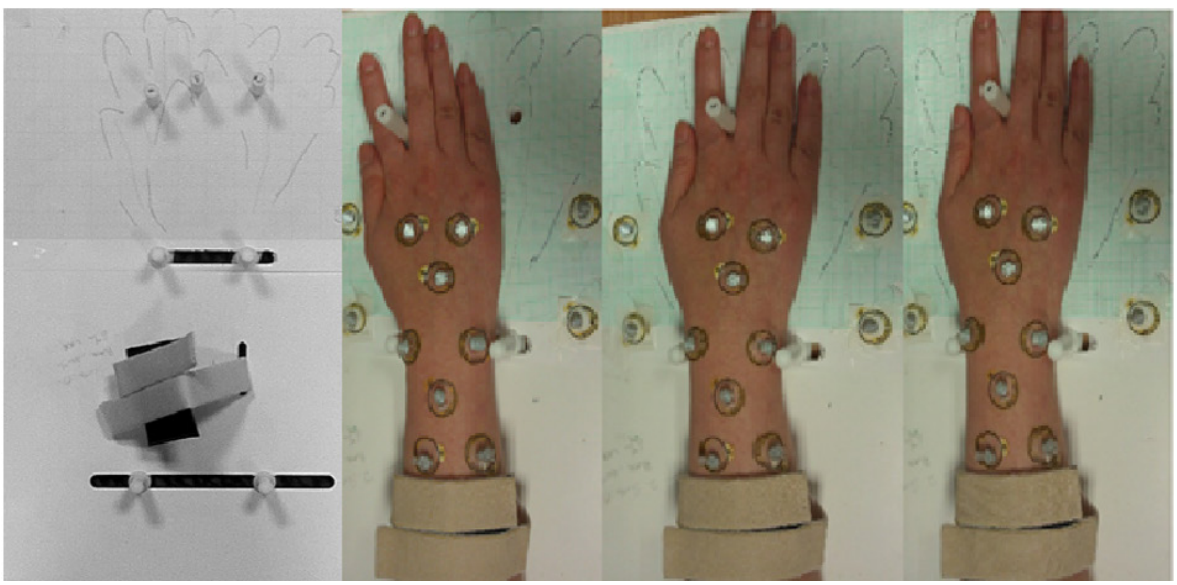

Figure 3. a) The jig used for b) stabilizing the predetermined positions of the hand and forearm marker locations during data collection in vivo.

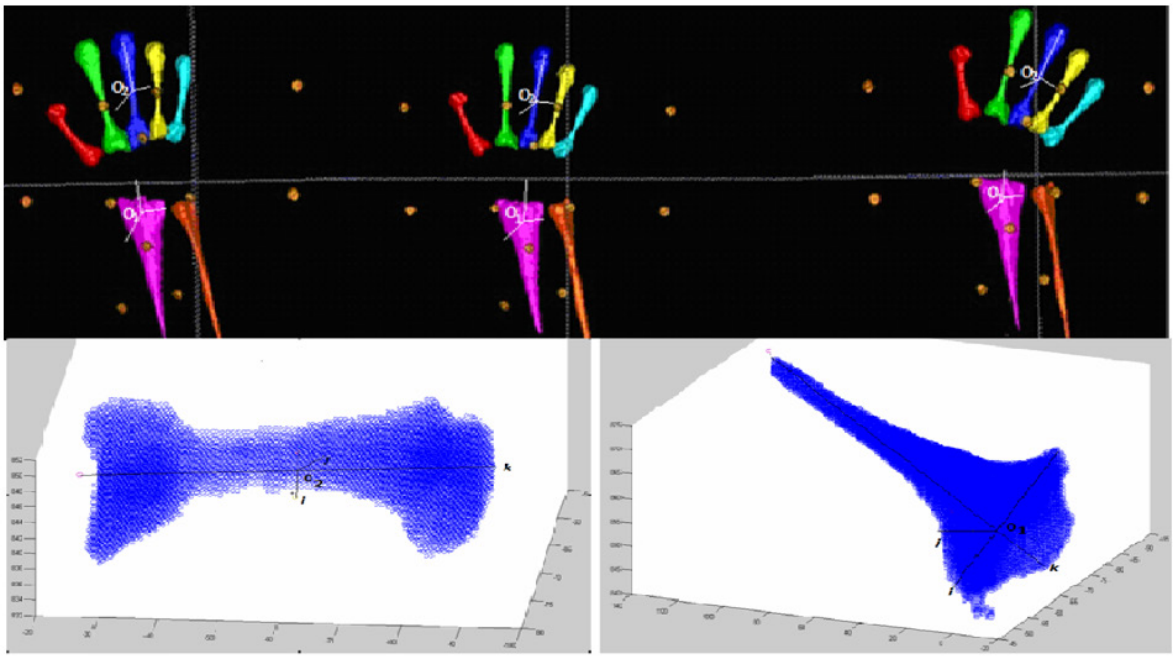

Figure 4. a) Adducted neutral and abducted postures of metacarpal, radius and ulna bones and external markers with coordinate centres shown based on PCA analysis b) Third metacarpal bone and c) radial bone information cloud derived from segmented images for PCA analysis.

MOCAP data outputs were recorded for the three different positions of the wrist.

For repeatability purposes, motion capture acquisition was repeated three times. Subjects were then taken to MRI unit with the markers still in situ and scanned in each of the three positions using the same MRI protocol as described previously. This three-position scan set was then repeated a second time to allow evaluation of reliability.

Post Processing

Image Processing

For the MOCAP data, the surface marker coordinate values were obtained directly from Visual 3D.

For the MRI images, the surface markers were isolated in the 3D image data by binarizing the image at a threshold selected by eye. Each connected component was then labelled and the centroid of each resulting labelled region was located using Snap ITK (Apache 2.0 license, Insight Software Consortium, NY, USA). The image was then registered to an arbitrary default grid using the versor based landmark transform algorithm of ITK (Apache 2.0 license, Insight Software Consortium, NY, USA) using the base markers (B1-4) to enable comparison with the MOCAP dataset.

For the in vivo phase, a manual segmentation process was undertaken to identify the metacarpal and radial bones in the MRI images of each of the six subjects (Fig. 4a). The third metacarpal bone and radial bone were selected to investigate the joint angle between the forearm and the hand. The segmented images of the two bones were converted to point-clouds and a principal component analysis was undertaken in MATLAB in order to consistently compute the origin and orientation of a coordinate system for each bone in each position (Fig. 4b,c). These coordinates were then used to calculate the joint angles of the bone.

Angular Calculations

The relative angles between the two links for the in vitro phase and the two bones for the in vivo phase were calculated using a bespoke code in MATLAB (version R2008a, The MathWorks Inc., USA) based on the coordinate data derived from the surface markers (MOCAP and MRI) and the segmented bones (MRI).

For the in vitro phase, two right handed reference frames, with orthogonal axes i, j and k, were defined on Link1 and Link2 (Fig. 2 a). The i and k directions were defined for each rigid body and the j vector was calculated as their cross-product. For reference frame1 (on the moving link frame Link 2), O_1 was defined as the average of the wrist markers (W1 and W2), the i vector was calculated as a vector from O_2 to W2 and the k vector as a line from O2 to centre of the H2 and H3 markers. For reference frame2 (on the fixed Link 1), O_2 was defined as average of wrist markers (F1 and F3), i was defined as a line from O1 to marker F3 and k as a line from O_2 to O_1 .

It was assumed that this local coordinate system was rigid and did not change during the movement, as the mar-

kers represent the rigid body corresponding to the logic of static measurements in Visual 3D. The i, j, and k directions were calculated for Link 2 as it rotated around Link 1, for the seven orientations at 30° intervals. The joint angle was defined by the relative orientation of one local coordinate system (H1-3) with respect to the other (F1-3) and was independent of the position of the origin of these coordinate systems.

For the in vivo phase, similar convention was used. PCA analysis provided the extreme points on the third metacarpal bone and the radial bone to use as internal bone marker co-ordinate data (Fig. 4). Centre of 3rd metacarpal bone was named as O_2 and centre of radial bone was named as O_1 (Fig. 4b). The k direction was defined as the line connecting the first component of third metacarpal bone O_2 and i direction was defined as the line connecting the second component of PCA to O_2. On radial bone k was defined from the centre of the first component of PCA to O_1 and i was defined as the line from the second component of PCA to O_1 (Fig. 4c).

Joint angles are rarely represented by an orientation matrix, but instead by a parameterized representation of this. A 3-D rotation matrix (in other words the orientation of one local coordinate system with respect to another) is represented by three successive rotations about unique axes. This ensures that three elements (angles) fully specify the nine components of a 3x3 rotation matrix. In this study, the rotation matrix was defined by multiplying the orientation matrix of the jig or wrist in two positions to calculate the joint angle. By elaborating the rotation matrix for the y-x-z sequence, the Cardan angles were extracted and designated α (alpha) for the first rotation, β (beta) for the second rotation, and γ (gamma) for the third rotation [11].

In order to validate the bespoke code written in MATLAB, initial post processing of the surface marker data with Visual 3D (C-Motion Inc, US) using an Y-X-Z Cardan sequence was undertaken to provide an industry standard benchmark. For the in vitro phase, the bespoke MATLAB and Visual 3D algorithms were used to calculate the angular rotation using both the MOCAP and MRI surface marker datasets. For the in vivo phase, to confirm that the code worked in the less constrained non-rigid system of natural wrist, the surface marker data (MRI) were fed back into Visual 3D. Rotational angular values were then calculated by using the Y-X-Z Cardan sequence in both Visual 3D and MATLAB and the outputs were compared.

Analysis

For the in vitro phase, the surface marker data from the MOCAP and MRI systems consisted of X, Y and Z coordinates. However, with a constrained jig, the Z coordinate was assumed to be constant for the surface markers on the two link mechanism. The translational (X, Y) coordinate data for the two modes of acquisition were compared by determining the root mean square (RMS) error for the seven different positions of Link 1. The results for angular rotation about the hinged axis were also compared between the two systems (Fig. 5), because this represents the relevant clinical output.

For the in vivo phase, the following comparisons were made:

a) Surface marker (MOCAP) data versus marker (MRI) data

The surface marker (MOCAP) data were deemed to constitute the best available gold standard for the lab-derived marker coordinates and the resulting angular rotations were calculated using Visual 3D (C-Motion Inc, US). These angles were compared with those derived from the surface marker (MRI) data, calculated using the bespoke MATLAB code to check if the systems were comparable irrespective of the input source data and code used. To determine the repeatability, the RMS error was also calculated for the repeated measurements undertaken using both MOCAP and MRI systems.

b) Surface marker (MRI) data versus segmented bone (MRI) data

The angular rotations calculated by the bespoke MATLAB code for the surface marker (MRI) data and segmented bone (MRI) data were compared. This was to determine the correlation between the bone and the surface markers when both measures were taken using the same (MRI) system.

c) Surface marker (MOCAP) versus segmented bone (MRI) data

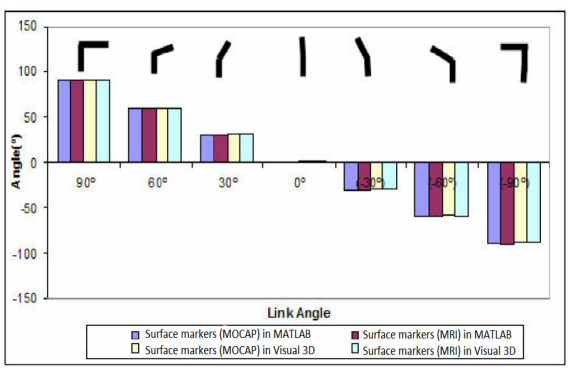

Figure 5. Calculated relative angle of Link1 with respect to Link2 using in-house MATLAB routines and Visual 3D based outputs for both MOCAP and MRI acquired data

Table 1. RMS difference between MRI and MOCAP data in (mm)

	Fixed markers (mm)									Rotating markers (mm)		
	B1	B2	B3	B4	F1	F2	F3	W1	W2	H1	H2	H3
X	0.19	0.15	0.24	0.42	0.29	0.45	0.61	0.23	0.33	0.51	0.69	0.31
Y	0.07	0.44	1.1	0.93	0.41	0.72	0.59	0.82	0.95	1.43	1.42	1.18

The outputs of Visual 3D for the surface markers (MOCAP) were compared with the outputs of the MATLAB code for the segmented bone (MRI) inputs. This was to represent the practical application of the method and determine if systematic errors existed between the two measurements that could be accounted for.

To assess the agreement between the two systems, mean-difference plots, a graphical method introduced by Bland & Altman [12], were derived for the angular values of the two segments relative to each other (Fig. 6). Finally, the concordance correlation coefficient was calculated as described by Lin [13] for angular data, providing a numerical indicator of agreement between the two acquisition protocols.

RESULTS

In Vitro

Marker Coordinates

The markers were analyzed in two sets; the fixed markers (B1 - B4, F1 - F3, W1 and W2) and the rotating markers attached to Link1 (H1 - H3). The maximum RMS errors for all the scan angles were found to be 0.69 mm and 1.43 mm in the X and Y directions respectively for all markers (Table1). The RMS errors were observed to be higher in the Y direction than in X both for fixed and rotating markers.

High levels of agreement were found between the marker positions determined from the MOCAP and MRI systems. Mean-Difference plots were constructed and the Concordance Correlation Coefficient (CCC) values were calculated separately for the X and Y coordinates. The mean of the differences was -0.18 ± 0.59 mm for the X direction and 0.66 mm ± 0.63mm for the Y direction. The CCC varied between 1 and 0.9998 for the fixed markers, and between 0.9999 and 0.9788 for the rotating markers.

Angular Rotations

The difference (RMS error) between the angular values determined from the MOCAP and MRI based data was found to be less than 1 °, with a maximum difference of 0.88° (Table 2). Good agreement was found between the in-house code and the proprietary Visual 3D output (Fig. 6a,b).

Table 2. Angular differences between MOCAP and MRI based data, both calculated using in-house code in MATLAB

Angular Difference between MOCAP and MRI Marker data(Matlab Derived)						
90°	60°	30°	0°	(-30°)	(-60°)	(-90°)
0.07	0.42	0.16	0.11	0.3	0.01	0.88

Mean-difference plots were constructed for angular values for the outputs from the MOCAP and MRI custom MATLAB routines. The RMS error was 0.05° (95% confidence interval= 0.39°) and the CCC for angular agreement between MOCAP and MRI data was 1.000.

In Vivo

The in-vivo data was derived from the mean of the outputs of the bespoke code and the gold-standard Visual 3D for the inputs of surface marker (MRI) data obtained from MRI scans in each position as explained in section 2.2.4 as a first step . To assess the agreement between the two systems, Bland & Altman plots were plotted for the angular values of the two segments relative to each other for abducted and adducted angles (Fig. 6b). Maximum angular difference was less than 1°. This showed that the MATLAB code calculates the angles not much different than the gold standard Visual 3D software for the less constrained system of natural wrist. Surface marker (MOCAP) versus (MRI) angle showed good agreement (Fig. 6b). CCC for adducted and abducted angular values between MATLAB and Visual 3D for the surface marker (MRI) data was 0.92 and 0.96 respectively. CCC was 0.97 and 0.98 for adduction an abduction respectively for the outputs of Visual 3D for the input data of Surface Markers (MOCAP) and outputs of MATLAB code for the surface markers (MRI).

The outputs of Visual 3D for the surface markers (MOCAP) were compared with the outputs of the MATLAB code for the segmented bone (MRI) inputs (Fig. 6c). Maximum RMS values were calculated for Visual 3D and MRI and segmented bone (MRI) data as 1.28°, 1.3°, and 0.98 ° respectively. This was to ensure the comparability of the bespoke code for reporting angular rotations when using

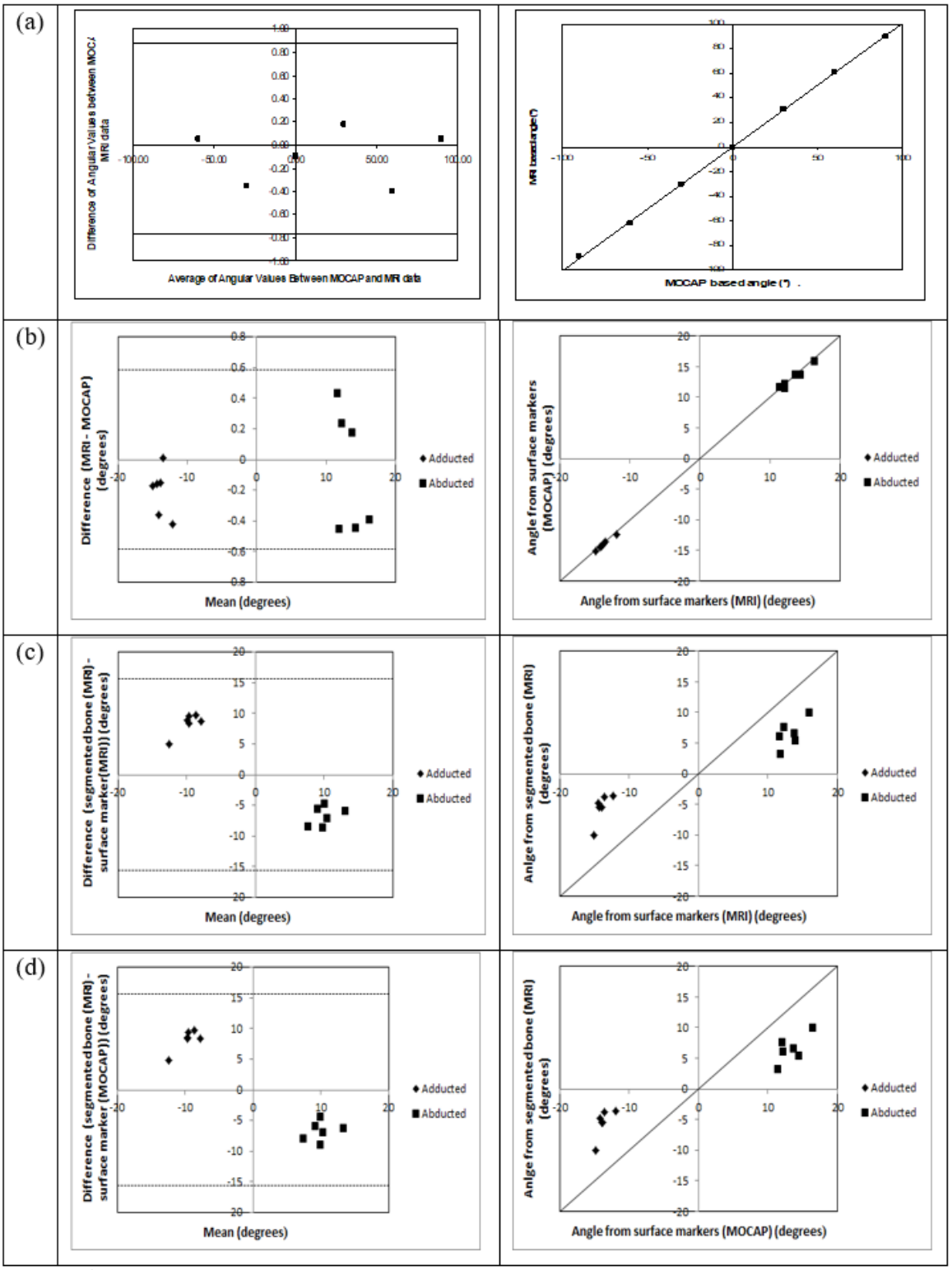

Figure 6. Difference-mean and agreement plots for (a) the in vitro phase and (b) to (d) the in vivo phase, showing the angular measurements calculated from (a) the MRI versus MOCAP marker jig positions; (b) the surface marker (MRI) versus the surface marker (MOCAP); (c) the bone segmentation (MRI) versus surface marker (MRI) and (d) the bone segmentation (MRI) versus surface marker (MOCAP).

markers visible in both MOCAP and MRI universes, so as to support the subsequent validity of data from the segmented bones which could not be cross-referenced to Visual 3D.

CCC was calculated as 0.05 and 0.1 between the outputs of Visual 3D for the input data of Surface Markers (MOCAP) and outputs of segmented bone (MRI) for adduction and ab-

duction respectively.

The outputs of MATLAB code for the input data of Surface Markers (MRI) and outputs of segmented bone (MRI) inputs were compared (Fig. 6d) CCC was calculated as 0.05 and 0.09 between the outputs of MATLAB code for the input data of surface Markers (MRI) and outputs of segmented bone (MRI) for adduction and abduction respectively.

A Student-t test for differences between the angular values calculated using surface markers (MOCAP) and segmentation of the internal bone (MRI) yielded a significant difference and therefore evidence of a systematic error for both adducted and abducted positions (p= 0.000095 p=0.000154 respectively). For both the adducted and abducted positions the angle derived from surface-mounted markers over-estimated the change in position of the underlying bony segment.

DISCUSSION

This study addressed the aim of establishing the proof of concept that marker coordinates derived independently using MRI and motion capture, could be accurately co-registered in a highly constrained system in vitro. Using an idealized environment, free from the confounding effect of skin movement artefact, the technical potential of the concept was demonstrated. Although both MRI and MOCAP systems are widely used in the field separately, when two systems are combined, the agreement between the data sets requires rigorous validation prior to use in clinical applications. Theoretical estimations are possible for the technical accuracy of the systems, but these estimates often relate poorly to real-world applications, due to confounders such as inhomogeneities in the magnetic field in MRI scanning and the orientation of the anatomy relative to the field [14].

Combination methods for internal imaging and motion capture have been described but only in abstract form to our knowledge [15] and there does not appear to be any peer reviewed literature formally investigating proof of concept and quantifying the associated errors.

To explore the differences between MRI and MOCAP systems quantitatively. I validated the data obtained from both systems using both bespoke MATLAB code (MATLAB version R2008a, The MathWorks Inc., USA) and Visual 3D (C-Motion Inc, US), the latter considered an industry standard. The novel code showed excellent agreement with the industry standard Visual 3D outputs in the in vitro phase, although we recognize that the benchmark itself will not be completely free of error. The in vivo study confirmed that there is a good agreement between Visual 3D and the MATLAB code in calculating outputs from the same surface marker inputs (MRI) despite the less constrained system.

For the in vitro study, in the absence of the possibility of surface movement relative to the rigid bodies, the MOCAP data represent the best available gold standard against which to compare the MRI outputs. Known sources of error in MR imaging, such as inhomogeneities in the main magnetic field and non-linearity in the applied magnetic field gradients are likely to have an effect when studying large volumes such as used in motion capture. The fixed markers yielded lower RMS error than rotating markers. Furthermore, the error along the Y axis, having a slightly higher systematic offset, was observed to be greater than for the X axis and largest at link position +/-90° when the rotating markers were at the greatest distance from the field iso-centre. In clinical applications for the wrist, neck or ankle it is likely that the ranges of motion would not exceed ± 45° and so this is the region in which the co-registration was required to be most accurate. In our study, for positions within ±60° of the longitudinal axis of the jig, the error in the coordinate data was less than 1 mm in both X and Y directions.

The concordance correlation coefficient results showed very high agreement between the MOCAP data and MRI data in the highly constrained in-vitro simulation. The CCCs for the estimates of surface marker coordinates were very high, and agreement between the two systems for angular rotation was effectively perfect. This provided confidence that, in a constrained system without the confounders of skin artefact, the two systems were able to predict highly similar outputs.

The relationship between surface marker (MOCAP) and segmented bone (MRI) data is similar for abducted and adducted postures. Student-t tests show that there is a significant difference between the angles calculated by surface markers (MOCAP) and internal segmented bone (MRI) data with the surface mounted markers significantly overestimating the rotations occurring in the underlying bony segments. This finding warrants further research as there is the potential to solve for systematic errors such as this is the over-estimation is predictable across a range of rotations or conditions.

One significant advantage of the co-registration of MRI and MOCAP universes is the elimination of the use of invasive techniques such as bone-mounted pin and unnecessary exposure ionising radiation. This would open up the technique to use in patient populations where study is limited due to ethical concerns.

Although this proof of concept study used the wrist

to represent a constrained rotation, there is potential to develop the technique for other joints, particularly joints in which surface mounted markers do not represent well the underlying bony segments. Although the field of view for accurate MRI scanning is limited due to increasing field inhomogeneity at the margins the 3D distortion correction algorithm provided a practically useful field of view in the current study. There is potential to map this further should a wider field of view be required.

I acknowledge that this proof of concept work focused solely on healthy subjects and as a minimum next-step prior to any clinical application, use of the technique to represent motions in the presence of pathological anatomy or function is required.

CONCLUSION

This study demonstrates the technical feasibility of using combination coated markers in both magnetic resonance imaging and optoelectronic motion capture universes, an approach that may have clinical applications for subject-specific studies subsequently.

In this study, the maximum magnitude of the error for the translational data in-vitro was less than 1.5 mm and for angular rotation, an accuracy of better than 1° was attained. In vivo the comparability of directly observed surface mounted markers was lower than in the in vitro simulations but remained within useful limits. A systematic difference was observed between the angles derived from the surface marker data and internal bone segments derived from MRI. Further studies are required to determine whether this systematic error is an intrinsic fault of MOCAP technologies using surface mounted markers. In the interim, care may be required in interpreting surface mounted marker data in terms of absolute values. It may be possible to solve for these differences on an individual basis but further work is required. It appears unlikely that a single correction factor could be applied which would be valid across different patients.

Prior to clinical applications where subject-specific kinematic models may provide insight into disease processes or treatment response models, this technique could now be evaluated in pathological states.

ACKNOWLEDGEMENT

The authors would like to thank to Dr. Richard Holbrey for this technical contribution to the marker registration algorithm.

CONFLICT OF INTEREST

Authors confirm there is no conflict of interest in this manuscript.

References

1. Strimpakos N 'The assessment of the cervical spine. Part 1: Range of motion and proprioception.' Journal of Bodywork and Movement Therapies 2011 15 ;1: 114-124
2. Andriacchi TP, Alexander EJ. 'Studies of human locomotion: past, present and future.' Journal of Biomechanics 2000 33:1217–1224.
3. Stagni, R., Fantozzi, S., Cappello, A., Leardini, A., 'Quantification of soft tissue artefact in motion analysis by combining 3D fluoroscopyand stereophotogrammetry: a study on two subjects.' ClinicalBiomechanics 2005; 20: 3; 320–329.
4. Jonsson, H., Karrholm, J., ' Three-dimensional knee joint movements during a step-up: evaluation after cruciate ligament rupture'. Journal of Orthopedic Research 1994; 12; 6: 769-779.
5. Reinschmidt, C., Borgert, A.J., van den, Nigg, B.M., Lundberg, A., Murphy, N., 'Effect of skin movement on the analysis of skeletal knee joint motion during running.' Journal of Biomechanics 1997; 30: 729-732.
6. Holden J, Orsini J, Siegel K, Kepple T, Gerber L, Stanhope S. Surface movements errors in shank kinematics and knee kinematics during gait. Gait and Posture 1997; 3:217–227.
7. Banks, S.A., Hodge, W.A., "Accurate measurement of three dimensional knee replacement kinematics using single-planefluoroscopy.' IEEE Transactions on Biomedical Engineering 1996; 43; 6 : 638-649.
8. Mundermann L, Corazza S, Andriacchi T, The evolution of methods for the capture of human movement leading to markerless motion capture for biomechanical applications. Journal of NeuroEngineering and Rehabilitation. 2006; 3; 6:1-11.
9. Alexander, E.J, Andriacchi, T.P., Lang, P.K Dynamic Functional Imaging of the Musculoskeletal System, Proceedings of the 1999 ASME Winter International Congress and Exposition, Nashville, Tennessee, November 1999; 14;19: 297-298.
10. Andersen S. Michael, Damsgaard M.,Rasmussen J, Ramsey D, ' Gait & Posture' 2012; 35; 606-611.
11. Joseph Hamill, W. Scott Selbie, and Thomas Kepple ' Unpublished book chapter from Visual 3D software group' Chapter 2 14. 2. 2011.
12. Bland M, Altman D G 'Statistical methods for assessing agreement. between two methods of clinical measurement'. Lancet 1986 ; 327; 8476: 307-310.
13. Lin, L I-Kuei 'Concordance Correlation Coefficient to Evaluate Reproducibility', Biometrics, 1989; 45;1: 255-268.
14. Stanescu T, Hans-Sonke J, Keith Wachowicz, B. Gino F 'Investigation of a 3D system distortion correction method for MR images'. Journal of Applied Clinical Medical Physics 2010; 11;1: 200-216.
15. Lang, P, Alexander, E.J, Andriachi, T.P. 'Functional joint imaging: A new technique integrating MRI and biomotion studies. International Society of Skeletal Radiology Annual Conference 2000.